

QA

1

B78

1983

V.2

TR/02/83

March 1983

Pole type singularities and the numerical  
conformal mapping

of

doubly-connected domains

by

N. Papamichael and M.K. Warby



per )  
QA  
:  
+  
B78

w9259998

## ABSTRACT

Let  $f$  be the function which maps conformally a given doubly-connected domain  $\Omega$  onto a circular annulus, and let

$$H(z) = f'(z)/f(z) - 1/z.$$

In this paper we consider the problem of determining the main singularities of the function  $H$  in  $\text{compl}(\Omega \cup \partial\Omega)$ . Our purpose is to provide information regarding the location and nature of such singularities, and to explain how this information can be used to improve the efficiency of certain expansion methods for numerical conformal mapping.



## 1. Introduction

Let  $\Omega$  be a finite doubly-connected domain with boundary  $\partial\Omega = \partial\Omega_1 \cup \partial\Omega_2$  in the complex  $z$ -plane, where  $\partial\Omega_i$ ,  $i = 1, 2$  are piecewise analytic Jordan curves. We assume that  $\partial\Omega_i$ ;  $i = 1, 2$  are respectively the inner and outer components of  $\partial\Omega$ , and that the origin  $0$  lies in the "hole" of  $\Omega$ , i.e.

$$0 \in \text{Int}(\partial\Omega_1).$$

Let  $t$  be a fixed point on  $\partial\Omega_1$  and let

$$w = f(z), \quad (1.1)$$

be the function which maps conformally  $\Omega$  onto the circular annulus

$$R = \{w: 1 < |W| < M\}, \quad (1.2)$$

so that  $f(t) = 1$ . The radius  $M$  of the outer circle is the so-called conformal modulus of  $\Omega$ .

This paper is concerned with the problem of determining the singularities of the function

$$H(z) = f'(z) / f(z) - 1/z, \quad (1.3)$$

in the complement of  $\bar{\Omega} = \Omega \cup \partial\Omega$ , i.e. the singularities of the analytic extensions of  $H$  in  $\text{Int}(\partial\Omega_1)$  and  $\text{Ext}(\partial\Omega_2)$ . The above problem may be re-garded as the generalization to the case of doubly-connected domains of the problem considered recently in [6], concerning the singularities of the analytic extension of the function that maps conformally a given simply-connected domain onto the unit

determine the numerical conformal map after first approximating the function  $H$  by means of a finite sum of the form

$$H_n(z) = \sum_{j=1}^n c_j \eta_j(z), \quad (1.4)$$

and the significance of knowing the singularities of  $H$  concerns the choice of the set of basis functions  $\{\eta_j(z)\}$ . More specifically, the practical significance of the work of the present paper emerges from the observation that the computational efficiency of the numerical mapping techniques improves considerably when the basis set contains terms that reflect the main singularities of  $H$  on  $\partial\Omega$  and in  $\text{compl}(\bar{\Omega})$ ; see [5].

Any singularities that  $H$  may have on  $\partial\Omega$  are corner singularities, and the problem for dealing with these is discussed fully in [5]. For this reason, in this paper we are concerned only with the singularities that  $H$  may have in  $\text{compl}(\bar{\Omega})$ . In particular, we are concerned with the behaviour of  $H$  at common symmetric points with respect to  $\partial\Omega_1$  and  $\partial\Omega_2$ , i.e. at pairs of points  $\zeta_1 \in \text{Int}(\partial\Omega_1)$  and  $\zeta_2 \in \text{Ext}(\partial\Omega_2)$  which are symmetric to each other with respect to both  $\partial\Omega_1$  and  $\partial\Omega_2$ . Such points play a very central role in the study of the singularities of the analytic extension of  $H$ . A simple example illustrating this is provided by considering the case where  $\Omega$  is the doubly-connected domain bounded by the two circles

$$\left. \begin{aligned} \partial\Omega_1 &= \{z : |z| = r_1\} \\ \partial\Omega_2 &= \{z : |z - a| = r_2\}, \quad |a| < r_1 - r_2. \end{aligned} \right\} \quad (1.5)$$

In this case the exact mapping function is

$$f(z) = k(z - \zeta_1)/(z - \zeta_2), \quad (1.6)$$

Where  $k$  is a constant such that  $|f(z)| = 1$ ,  $z \in \partial\Omega_1$ , and  $\zeta_1, \zeta_2$  are

Common symmetric with respect to the two circles (1.5), i.e.  $\zeta_1$  and  $\zeta_2$  satisfy the equations

$$\text{and } \left. \begin{aligned} \zeta_1 \overline{\zeta_2} &= r_1^2 \\ (\zeta_1 - a) \overline{(\zeta_2 - a)} &= r_2^2 . \end{aligned} \right\} \quad (1.7)$$

This means that

$$H(z) = 1/(z - \zeta_1) - 1/(z - \zeta_2) - 1/2, \quad (1.8)$$

i.e.  $H$  has a simple pole at each of the points  $\zeta_1$  and  $\zeta_2$ .

In the present paper we consider more general geometries than that defined by (1.5) and show that, under certain conditions, common symmetric points are again singular points of the function  $H$ . Unfortunately, in the case of a more general  $\Omega$ , we do not know the precise nature of the singularities of  $H$ . However, for the purposes of the numerical mapping techniques, our results suggest strongly that the singular behaviour of  $H$  may be reflected approximately by introducing into the basis set  $\{\eta_j(z)\}$  functions corresponding to simple poles at the common symmetric points.

The details of the presentation are as follows. In Section 2 we consider in detail the case where  $\Omega$  is a regular polygon with a circular hole. The study of this special, but non-trivial, geometry leads naturally to the study of more general geometries in Section 3. Finally, in Section 4 we present several numerical examples illustrating the importance of our results, in connection with expansion methods for numerical conformal mapping. In each of these examples the approximations to  $H$ , and hence to the mapping function  $f$ , are computed by using the orthonormalization method studied recently in [5].

## 2. Regular Polygon with Circular Hole

In this section we consider in detail the case where the inner boundary  $\partial\Omega_1$  of  $\Omega$  is the circle  $|z| = a$ ,  $a < 1$ , and the outer boundary  $\partial\Omega_2$  is a concentric  $n$ -sided regular polygon with short radius (apothem) unity. We assume, without loss of generality, that the polygon  $\partial\Omega_2$  is orientated so that one of its sides the side  $AC$ , is bisected by the real axis at the point  $B = (1,0)$  and, referring to Fig. 2.1(a), we let

$$r_1 = \text{arc } DF = \{z : z = ae^{i\theta}, |\theta| \leq \pi/n\} \quad (2.1)$$

and

$$r_2 = \overline{AC} = \{z : z = 1 + iy, |y| \leq \tan(\pi/n)\} \quad (2.2)$$

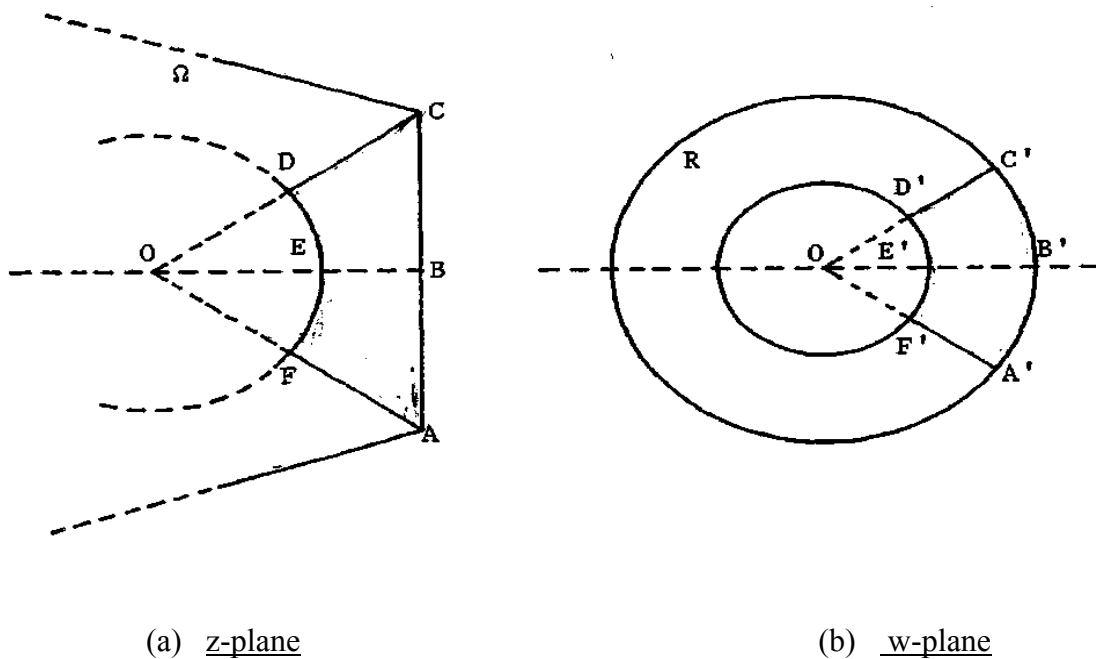


FIGURE 2.1



Let

$$W=f(z), \quad (2.3)$$

With  $f(a) = 1$ , be the function which maps conformally  $\Omega$  on to the circular annulus

$$R=\{w:1<|W|<M\}, \quad (2.4)$$

and let  $G$  denote the shaded region of Fig. 2.1(a), i.e. the region bounded by  $\Gamma_1, \Gamma_2$  and the two rays  $\theta = \pm\pi/n$ . Then, because of the  $2n$ -fold symmetry of  $\Omega$ , the function  $f$  maps  $G$  conformally onto the sector

$$G' = \{w : w = \rho e^{i\theta}, 1 < \rho < M, |\theta| < \pi/n\}, \quad (2.5)$$

so that the straight line  $EB$ , joining the points  $(a,0)$  and  $(1,0)$  goes onto the straight line  $E'B'$ , joining the points  $(1,0)$  and  $(M,0)$ ; see Fig. 2.1 (b).

As was previously remarked, the purpose of this section is to examine the behaviour of the analytic extension of the function

$$H(z) = f'(z) / f(z) - 1/z, \quad (2.6)$$

near the two common symmetric points with respect to  $r_1$  and  $r_2$ . In order to do this, we need to introduce some additional notation and to establish the preliminary results contained in Lemma 2.1.

Let  $I_1(z)$  and  $I_2(z)$  define respectively the symmetric points, of a point  $z$ , with respect to the circle  $|z| = a$  and the straight line  $x = 1$ , ie.

$$I_1(z) = a^2/\bar{z} \quad \text{and} \quad I_2(z) = 2 - \bar{z}. \quad (2.7)$$

Also let

$$S_1 = I_1 \circ I_2 \quad \text{and} \quad S_2 = I_2 \circ I_1, \quad (2.8)$$

so that

$$S_1(z) = a^2/(2-z)$$

(2.9)

and

$$S_2(Z) = 2-a^2/z$$

(2.10)

define respectively the symmetric points of  $I_2(z)$  with respect to the circle  $|z| = a$  and of  $I_1(z)$  with respect to the straight line  $x = 1$ .

Then, the common symmetric points  $\zeta_1 \in \text{Int}(\partial\Omega_1)$  and  $\zeta_2 \in \text{Ext}(\partial\Omega_2)$ , with respect to  $\Gamma_1$  and  $\Gamma_2$ , are fixed points of both functions  $S_j$ ;  $j = 1, 2$ . That is,  $\zeta_1$  and  $\zeta_2$  are the roots of the quadratic equation

$$Z^2 - 2Z + a^2 = 0, \quad (2.11)$$

i.e.

$$\zeta_1 = 1 - (1 - a^2)^{\frac{1}{2}} \quad \text{and} \quad \zeta_2 = 1 + (1 - a^2)^{\frac{1}{2}}. \quad (2.12)$$

Lemma 2.1

Let  $\zeta_1$  and  $\zeta_2$  be the common symmetric points (2.12), and define recursively the two point sequences  $\{z_{k,j}\}$ ;  $j = 1, 2$  by means of

$$Z_{k+1,j} = S_j(z_{k,j}); \quad k = 1, 2, \dots \quad (2.13)$$

Then, the following results hold.

$$(i) \quad \text{For any } z_{0,j} \in \overline{G}, \quad \lim_{k \rightarrow \infty} z_{k,j} = \zeta_j; \quad j = 1, 2, \quad (2.14)$$

and, in each case, the convergence is linear.

(ii) The mapping function  $f$  can be continued analytically across  $\Gamma_1$  and  $\Gamma_2$  into two regions  $G(\Gamma_1)$  and  $G(\Gamma_2)$  which contain respectively the

real intervals  $\zeta_1 < x < a$  and  $1 < x < \zeta_2$ .

(iii) For any  $z_{0,j} \in \overline{G}$ ,

$$\lim_{k \rightarrow \infty} f(z_{k,1}) = 0 \quad \text{and} \quad \lim_{k \rightarrow \infty} f(z_{k,2}) = \infty . \quad (2.15)$$

### Proof

(i) The result is established by using the identities

$$\{S_j(z) - S_j(\zeta_j)\} / (z - \zeta_j) = \begin{cases} \zeta_1 / (2 - z), & \text{if } j=1, \\ \zeta_1 / z & \text{if } j=2. \end{cases} \quad (2.16)$$

These imply that

$$|z_{k+1,j} - \zeta_j| \leq \zeta_1^k |z_{0,j} - \zeta_j| ; \quad j = 1, 2, \quad k \geq 0 , \quad (2.17)$$

and hence the convergence of the two sequences to  $\zeta_1$  and  $\zeta_2$  respectively. That the convergence is linear follows at once from the observation that

$$\lim_{k \rightarrow \infty} \left[ \{z_{k+1,j} - \zeta_j\} / \{z_{k,j} - \zeta_j\} \right] = S'_j(\zeta_j) ; \quad j = 1, 2 , \quad (2.18)$$

where

$$S'_j(\zeta_j) = (a / \zeta_2)^2 ; \quad j = 1, 2 . \quad (2.19)$$

(ii) The proof is based on the repeated application of the Schwarz reflection principle. This principle shows that the function  $f$  can be continued analytically across  $\Gamma_1$  and  $\Gamma_2$  by means of

$$f(I_1(z)) = 1/\overline{f(z)} \quad \text{and} \quad f(I_2(z)) = M^2/\overline{f(z)}, \quad z \in G \quad (2.20)$$

Then, for any  $k \geq 0$ ,  $f$  can be continued recursively into two regions

$G_{k+1}(\Gamma_j); j = 1, 2$ , which contain respectively the points  $z_{k+1,j}; j = 1, 2$ , by means

$$\text{and } \left. \begin{aligned} f(s_1(z)) &= f(z)/M, & z \in G_k(\Gamma_1), \\ f(s_2(z)) &= M^2 f(z), & z \in G_k(\Gamma_2), \\ & & k=0, 1, 2, \dots \end{aligned} \right\} \quad (2.21)$$

where  $G_0(\Gamma_1) = G_0(\Gamma_2) = G$ . Therefore, because of (2.14),  $f$  can be continued into two regions  $G(\Gamma_j); j = 1, 2$ , which contain respectively the intervals  $\zeta_1 < x < a$  and  $1 < x < \zeta_2$ .

(iii) The equations (2.21) imply that

$$f(z_{k+1,1}) = f(z_{k,1})/M^2 \quad \text{and} \quad f(z_{k+1,2}) = M^2 f(z_{k,2}), \quad k \geq 0. \quad (2.22)$$

Since  $M > 1$ , the result (2.15) follows at once from (2.22) and (2.14).

In particular we observe that

$$\lim_{x \downarrow \zeta_1} f(x) = 0 \quad \text{and} \quad \lim_{x \downarrow \zeta_2} f(x) = \infty.$$

This is established by taking the points  $z_{0,j}; j = 1, 2$  to be real.

Our main result concerning the behaviour of the function  $H$  near the common symmetric points  $\zeta_1$  and  $\zeta_2$  is contained in the following theorem.

Theorem 2.1

et  $\{z_{k,,j}\}; j = 1, 2$ , be the two sequences defined by (2.13) and let  $H$  be the function (2.6). Then for any  $z_{0,j} \in \overline{G}$ ,

$$\lim_{k \rightarrow \infty} \{(z_{k,j} - \zeta_j)H(z_{k,j})\} = \lambda_j; \quad j=1, 2 \quad (2.23)$$

where  $\lambda_1$  and  $\lambda_2$  are finite and, in general, non-zero numbers which depend respectively on the points  $z_{0,1}$  and  $z_{0,2}$ .

Proof

Let

$$\phi(z) = f'(z)/f(z) \quad , \quad (2.24)$$

and

$$e_{k,j} = z_{k,j} - \zeta_j \quad . \quad (2.25)$$

Then from (2.21) and (2.22),

$$\phi(z_{k+1,j}) S'_j(z_{k,j}) = \phi(z_{k,j}); \quad j=1,2, k \geq 0, \quad (2.26)$$

and, from (2.16),

$$e_{k+1,j} = e_{k,j} g_j(z_{k,j}); \quad j=1,2 \quad , \quad (2.27)$$

where  $g_1(z) = \zeta_1/(2-z)$  and  $g_2(z) = \zeta_2/z$ . Thus

$$\begin{aligned} e_{k+1,j} \phi(z_{k+1,j}) &= \{g_j(z_{k,j})/S'_j(z_{k,j})\} e_{k,j} \phi(z_{k,j}) \\ &= (1+c_j e_{k,j}) e_{k,j} \phi(z_{k,j}) \\ &= \left\{ \prod_{m=0}^k (1+c_j e_{m,j}) \right\} e_{0,j} \phi(z_{0,j}); \quad j=1,2, \end{aligned} \quad (2.28)$$

where  $c_1 = 1/(2 - \zeta_1)$  and  $c_2 = 1/\zeta_2$ . Because of (2.18)-(2.19), D' Alembert 's ratio test shows that the series  $\sum |e_{m,j}|$ ;  $j = 1,2$ , converge and this in turn implies that

$$\lim_{k \rightarrow \infty} \left\{ \prod_{m=0}^k (1+c_j e_{m,j}) \right\} = \alpha_j ; \quad j=1,2, \quad (2.29)$$

where  $\alpha_1$  and  $\alpha_2$  are finite and non-zero numbers; see e.g. Henrici [3,p.4].

Therefore, from (2.28)-(2.29),

$$\lim_{k \rightarrow \infty} e_{k,j} H(z_{k,j}) = \lim_{k \rightarrow \infty} e_{k,j} \phi(z_{k,j}) = \lambda_j ; j = 1, 2 , \quad (2.30)$$

where

$$\lambda_j = \alpha_j e_{0,j} \phi(z_{0,j}) \quad (2.31)$$

(That the constants  $\lambda_j$  depend on  $z_{0,j}$  can be seen by observing that if  $z_{0,j} \in G$  then  $\lambda_j \neq 0$ . However, if  $z_{0,j}$  is one of the corners A or C of  $\partial\Omega_2$  then  $\lambda_j = 0$ , because in this case  $\phi(z_{0,j}) = 0$ .)

Theorem 2.1 shows that the common symmetric points with respect of  $\Gamma_1$  and  $\Gamma_2$  are "singular" points of H, and provide the only information we have regarding the behaviour of H at  $\zeta_1$  and  $\zeta_2$ . The theorem suggests that it might be possible to reflect approximately the singular behaviour of H by that of two simple poles at  $\zeta_1$  and  $\zeta_2$ .

It is of interest to observe that if H did have simple poles at  $\zeta_1$  and  $\zeta_2$ , with residues  $r_1$  and  $r_2$  respectively, then near the two symmetric points the mapping function f would have behaved like the multivalued function

$$(z - \zeta_j)^{r_j} ; j = 1, 2 . \quad (2.32)$$

Furthermore, from (2.22) and (2.18)-(2.19), the values  $r_1$  and  $r_2$  in (2.32) would have satisfied

$$r_1 = -r_2 = \log M / \log(\zeta_2 / a) . \quad (2.33)$$

The above lead us to conjecture that the behaviour of f near the common symmetric points is reflected approximately by (2.32) - (2.33). This conjecture is supported by the following theorem.

Theorem 2.2

Let  $\{z_{k,j}\}; j = 1,2$ , be the two sequences defined by (2.13) and let  $r_1$  and  $r_2$  be given by (2.33). Then for any  $z_{0,j} \in \overline{G}$ ,

$$\lim_{k \rightarrow \infty} \left\{ (z_{k,j} - \zeta_j)^{-r_j} f(z_{k,j}) \right\} = \mu_j ; j = 1,2 , \quad (2.34)$$

Where  $\mu_1$  and  $\mu_2$  are finite and non-zero numbers which depend respectively on the points  $z_{0,1}$  and  $z_{0,2}$ .

Proof

The Equations (2.27) may be written as

$$e_{k+1,j} = \psi_j(e_{k,j}) ; j = 1, 2 , \quad (2.35)$$

where

$$\psi_j(z) = \zeta_1 z / \{ \zeta_2 + (-1)^j z \} ; j = 1, 2 . \quad (2.36)$$

Let the functions  $\psi_j^{(k)}$  be defined recursively by means of

$$\psi_j^{(1)} = \psi_j , \psi_j^{(k+1)} = \psi_j \circ \psi_j^k ; k = 1,2,\dots , \quad (2.37)$$

so that

$$e_{k,j} = \psi_j^{(k)}(e_{0,j}) ; k = 1,2,\dots, j = 1,2 , \quad (2.38)$$

where by induction,

$$\psi_j^{(k)} = (\zeta_1/\zeta_2)^k \left\{ z / (1 + (-1)^j b_k z) \right\} , \quad (2.39)$$

with

$$b_k = \left\{ 1 - (\zeta_1/\zeta_2)^k \right\} / (\zeta_2 - \zeta_1) . \quad (2.40)$$

Since, from (2.22),

$$f(z_{k,j}) = (M^{2k})^{(-1)^j} f(z_{0,j}) , \quad (2.41)$$

it follows from (2.38) and (2.39) that

$$e_{k,j}^{-r} f(z_{k,j}) = \left\{ e_{0,j} / (1 + (-1)^j b_k e_{0,j}) \right\}^{-r} \left\{ (\zeta_1 / \zeta_2)^{-r} (M^2)^{(-1)^j} \right\}^k f(z_{0,j}) \quad . \quad (2.42)$$

But, from (2.33),

$$(\zeta_1 / \zeta_2)^{-r_1} = (\zeta_1 / \zeta_2)^{-r_2} = M^2 \quad ,$$

and therefore

$$e_{k,j}^{-r} f(z_{k,j}) = \left\{ e_{0,j} / (1 + (-1)^j b_m e_{0,j}) \right\}^{-r} f(z_{0,j}) \quad . \quad (2.43)$$

Since

$$\lim_{k \rightarrow \infty} b_k = 1/2(1 - a^2)^{\frac{1}{2}} \quad ,$$

the result (2.34) follows at once from (2.43).

We end this section by establishing a result which indicates that the functions (2.32) - (2.33) reflect more closely the behaviour of  $f$  at the common symmetric points, when the radius  $a$  of  $\partial\Omega_1$  is close to unity. We do this as follows.

Let

$$t_0 = a^2 \sec(\pi/u) \quad , \quad t_1 = \sec(\pi/u) \quad , \quad (2.44)$$

and let the sequence of functions  $\{z_{k,1}(t)\}$  be defined recursively

by means of

$$\left. \begin{aligned} z_{0,1}(t) &= t \exp(i\pi t / u) \quad , \quad t_0 \leq t \leq t_1 \\ z_{k+1,1}(t) &= S_1(z_{k,1}(t)) \quad ; \quad k = 0, 1, 2, \dots \quad , \end{aligned} \right\} \quad (2.45)$$



where  $S_1$  is the function (2.9). Then, referring to Fig. 2.1(a),

$$L_0 = \{z : z = z_{0,1}(t) \quad , \quad t_0 \leq t \leq t_1\}$$

is the straight line segment joining the point  $t_0 \exp(i\pi/n)$  to the point C and, from the proof of Lemma 2.1,

$$C_k = \{z : z = z_{k,1}(t) \quad , \quad t_0 \leq t \leq t_1\} ; \quad k = 1, 2, 3, \dots ,$$

is an infinite sequence of circular arcs whose union

$$J = \bigcup_{i=1}^{\infty} C_k ,$$

forms part of the boundary of the region  $G(\Gamma_1)$ . Let  $G$  be the region bounded respectively by the straight line  $L_0$ , the curve  $J$ , the straight line  $L_1$  joining the common symmetric point  $\zeta_1$  to the point  $B = (1,0)$ , and the straight line  $\overline{BC}$ ; see Fig. 2.1(a). Then, the function  $f$  maps  $G$  onto the sector

$$OA'c' = \{w : 0 < |w| < M \quad , \quad 0 < \arg w < \pi/n\}$$

so that the straight line  $L_1$  and the curve  $L_0 \cup J$  go respectively onto the radial lines  $OE'B'$  and  $OD'C'$  of Fig. 2.1(b).

The above suggest that it might be possible to determine how closely (2.32)-(2.33) reflect the behaviour of  $f$  at  $\zeta_1$  and  $\zeta_2$  by considering the function

$$Q(t) = \lim_{k \rightarrow \infty} \arg (z_{k,1}(t) - \zeta_1) \quad , \quad -\pi < \arg(\bullet) \leq \pi \quad , \quad (2.46)$$

and determining constants  $\alpha$  and  $\beta$  such that, for all  $t \in [t_0, t_1]$ ,

$$\alpha \leq Q(t) \leq \beta \quad . \quad (2.47)$$

More precisely, the motivation for using (2.47) as a criterion emerges

from the observation that if  $f$  had the behaviour (2.32)-(2.33) then the curve which is mapped by  $f$  onto the straight line  $OE'B'$  would have had a tangent at the point  $\zeta_1$ . Furthermore this tangent would have been inclined at an angle

$$\theta = \pi/r_1 n \quad (2.48)$$

to the real axis and, for all  $t \in [t_0, t_1]$ , the function  $Q$  would have satisfied

$$Q(t) = \theta . \quad (2.49)$$

### Theorem 2.3

Let  $t_0, t_1$  be given by (2.44). Then, for any  $t \in [t_0, t_1]$ , the function  $Q$  of (2.46) satisfies

$$\alpha \leq Q(t) \leq \beta , \quad (2.50)$$

where

$$\alpha = Q(a) = \arg \{ (\cos(\pi/n) - a + i(1-a^2)^{\frac{1}{2}} \sin(\pi/n)) \} \quad (2.51)$$

and

$$\beta = Q(t_0) = \arg \{ \cos(2\pi/n) - a^2 \cos^2(\pi/n) + 2i(1-a^2)^{\frac{1}{2}} \sin(2\pi/n) \} . \quad (2.52)$$

Furthermore,

$$\lim_{a \rightarrow 0^+} \alpha = \pi/n , \quad \lim_{a \rightarrow 0^+} \beta = 2\pi/n , \quad (2.53)$$

and

$$\lim_{a \rightarrow 1^-} \alpha = \lim_{a \rightarrow 1^-} \beta = \pi . \quad (2.54)$$

Proof

By using (2.12) and (2.38)-(2.40), it can be shown that

$$Q(t) = \arg(\text{texp}(i\pi/n) - \zeta_1) + \arg(\zeta_2 - \text{texp}(-i\pi/n)) . \quad (2.55)$$

The theorem follows easily from (2.55).

Theorem 2.33 shows that when  $a$  is close to unity then the functions (2.32)-(2.33) reflect more closely the behaviour of  $f$  at  $\zeta_1$  and  $\zeta_2$ , in the sense that the difference  $\beta - \alpha$  of the two constants in (2.50) tends to zero as  $a \rightarrow 1^-$ . Furthermore the theorem, in conjunction with (2.48)-(2.49), suggests that  $r_1$  might satisfy

$$\pi/n\beta \leq r_1 \leq \pi/n\alpha . \quad (2.56)$$

3. Other Geometries

Let  $\Gamma$  be an analytic arc with parametric equation

$$z = \tau(s), \quad s_1 < s < s_2 . \quad (3.1)$$

Then, for any point  $z$  sufficiently close to  $\Gamma$ ,

$$I(z) = \tau\{\overline{\tau^{-1}(z)}\}$$

defines a symmetric point of  $z$  with respect to  $\Gamma$ ; see e.g.

Sansone and Gerretsen [8,p.103]. Let now  $\Gamma_j \subseteq \partial\Omega_j$ ;  $j = 1,2$ , be

two analytic arcs of the boundary  $\partial\Omega = \partial\Omega_1 \cup \partial\Omega_2$  of a doubly—connected

domain . Also, let  $I_j(z)$ ;  $j = 1,2$ , be the functions corresponding

to (3.2), which define respectively pairs of symmetric points

$(z, I_j(z))$ ;  $j = 1,2$ , with respect to the arcs  $\Gamma_j$ ;  $j = 1,2$ . Then,

as in the case of the special geometry considered in Section 2, the

points  $\zeta_1 \in \text{Int}(\partial\Omega_1)$  and  $\zeta_2 \in \text{Ext}(\partial\Omega_2)$  are said to be common symmetric

points with respect to  $\Gamma_1$  and  $\Gamma_2$  if

$$\zeta_1 = I_j(\zeta_2) \quad \text{and} \quad \zeta_2 = I_j(\zeta_1); \quad j=1,2, \quad (3.3)$$

i.e.  $\zeta_1$  and  $\zeta_2$  are common symmetric points if they are both fixed points of the two composite functions

$$S_1 = I_1 \circ I_2 \quad \text{and} \quad S_2 = I_2 \circ I_1. \quad (3.4)$$

Of course the points  $\zeta_1$  and  $\zeta_2$  may not exist. (For example, there are no common symmetric points with respect to two straight line segments  $\Gamma_1$  and  $\Gamma_2$ .) Here we assume that  $\zeta_1$  and  $\zeta_2$  exist, and also make a number of additional assumptions. Our assumptions are as follows:

A1: The arcs  $\Gamma_1$  and  $\Gamma_2$  are such that the common symmetric points  $\zeta_1$  and  $\zeta_2$  exist.

A2: There exists some region  $G \in \overline{\Omega}$ , partly bounded by  $\Gamma_1$  and  $\Gamma_2$ , so that for any  $z_{0,j} \in \overline{G}$

$$\lim_{k \rightarrow \infty} z_{k,j} = \zeta_j; \quad j = 1,2, \quad (3.5)$$

where the two point sequences  $\{z_{k,j}\}; j = 1,2$ , are defined, as in Section 2, by means of

$$z_{k+1,j} = s_j(z_{k,j}) \quad ; \quad k = 0,1,2,\dots. \quad (3.6)$$

A3: The rate of convergence of each of the two sequences (3.6) to  $\zeta_1$  and  $\zeta_2$  is at least linear.

A4: The two functions  $S_1$  and  $S_2$  are analytic at the points  $\zeta_1$  and  $\zeta_2$  respectively.

We observe that the assumption A4 implies that

$$S_1'(\zeta_1) = \overline{S_2'(\zeta_2)}, \quad (3.6)$$

and that

$$S_j(z) - S_j(\zeta_j) = (z - \zeta_j)^{n_j} g_j(z); j=1,2. \quad (3.7)$$

where  $n_j = 1$  if  $S_j'(\zeta_j) \neq 0$ ,  $n_j > 1$  if  $S_j'(z_j) = 0$  and where the functions  $g_j$ ;  $j=1,2$  are analytic and non-zero at the points  $\zeta_j$ ;

$j=1,2$ , respectively. Clearly, because of (3.6), the integers  $n_j$  in (3.7) are either  $n_1 = n_2 = 1$  or  $n_j > 1$ ;  $j=1,2$ ,

As in Section 2, we let

$$e_{k,j} = z_{k,j} - \zeta_j, \quad (3.8)$$

and

$$H(z) = \varphi(z) - 1/z, \quad \varphi = f'/f, \quad (3.9)$$

where  $f$  is the function that maps  $\Omega$  conformally onto the circular annulus (2.4) so that  $f(t) = 1, t \in \partial\Omega_1$ . Then, corresponding to Theorem 2.1, we have the following.

### Theorem 3.1

Under the assumptions A1 - A4, the following results hold.

(i) If  $S_j'(\zeta_j) \neq 0$ ;  $j=1,2$  then, for any  $z_{0,j} \in \overline{G}$ ,

$$\lim_{k \rightarrow \infty} \{(z_{k,j} - \zeta_j)H(z_{k,j})\} = \lambda; \quad j=1,2, \quad (3.10)$$

where the constants  $\lambda_1$  and  $\lambda_2$  are finite and, in general, non-zero.

(ii) If  $S_j'(\zeta_j) = 0$ ;  $j=1,2$ , then, for any  $z_{0,j} \in \overline{G}$

$$\lim_{k \rightarrow \infty} \{(z_{k,j} - \zeta_j)H(z_{k,j})\} = 0; \quad j=1,2, \quad (3.11)$$

and

$$\lim_{k \rightarrow \infty} \left\{ |z_{k,j} - \zeta_j| \log |z_{k,j} - \zeta_j| \left| H(z_{k,j}) \right| \right\} = \mu_j ; j=1,2, \quad (3.12)$$

where the constants  $\mu_1$  and  $\mu_2$  are finite and, in general, non-zero.

Proof

The proof is similar to that of Theorem 2.1. Thus, from (3.7),

$$e_{k+1,j} = e_{k,j}^{n_j} g_j(z_{k,j}); \quad j=1,2, \quad k \geq 0, \quad (3.13)$$

$$S_j^k(z_{k,j}) = e_{k,j}^{n_j-1} \{ n_j g_j(z_{k,j}) + e_{k,j} g_j'(z_{k,j}) \}; \quad j=1,2, \quad k \geq 0, \quad (3.14)$$

and hence, because of (2.26),

$$e_{k+1,j} \phi(z_{k+1,j}) = \{ 1/n_j + 0(e_{k,j}) \} e_{k,j} \phi(z_{k,j}) \\ = \left\{ \prod_{m=0}^k (1/n_j + 0(e_{m,j})) \right\} e_{0,j} \phi(z_{0,j}); \quad j=1,2, \quad k \geq 0. \quad (3.15)$$

Since

$$\lim_{k \rightarrow \infty} \left\{ \prod_{m=0}^k (1/n_j + 0(e_{m,j})) \right\} = \begin{cases} a_{j \neq 0}, & \text{if } n_j = 1, \\ 0, & \text{if } n_j > 1, \end{cases} \quad (3.16)$$

the results (3.10) and (3.11) follow at once from (3.9) and (3.15).

The result (3.12) also follows from (3.15) - (3.16) by observing that

$$\log |e_{k+1,j}| = n_j \log |e_{k,j}| + \log |g_j(z_{k,j})|. \quad (3.17)$$

Theorem 3.1 extends the results of Section 2, concerning the singular behaviour of  $H$  at common symmetric points, to more general doubly-connected domains than polygons with circular holes .

Corresponding to the formula (2.33) we now have that

$$r_1 = -\bar{r}_2 = 2 \log M / \log \{ S_1^k(\zeta_1) \}, \quad (3.18)$$

where the principal value of the logarithm is taken. That is, in the case of a general  $f_i$ , if the function  $H$  did have simple poles at  $\zeta_1, \zeta_2$  then, by taking  $n_1 = n_2 = 1$  and using (2.2), (3.6) and (3.7), it can be shown that the residues  $r_1, r_2$  of these poles would have satisfied (3.18).

Although, in general, it might be difficult to verify rigorously the assumptions A1 -A4, there are many geometries for which the common symmetric points may be determined easily. To illustrate this we consider below the two cases where  $\Omega$  is respectively an elliptical domain with a circular hole and a circular domain with a "cardioid shaped" hole.

### 3.1 Elliptical domain with circular hole

Let  $\Omega$  be the doubly-connected domain whose interior and exterior boundaries are respectively

$$\partial\Omega_1 = \{(x, y) : x^2 + y^2 = a^2/9\}, \quad (3.19)$$

and

$$\partial\Omega_2 = \{(x, y) : (x + a/2)^2/a^2 + y^2 = 1\} \quad 1 < a \leq 2,$$

and let  $\Gamma_j = \partial\Omega_j$ ;  $j=1,2$ ; Fig. 3.1. Then

$$I_1(z) = a^2/9\bar{z}, \quad (3.20)$$

and, from [ 7, Eq. (3.8) ],

$$I_2(z) = -a/2 + \{(\bar{a}^2 + 1)(\bar{z} + a/2) + 2ia(\bar{a}^2 - 1 - (\bar{z} + a/z)^2)^{1/2}\}/(\bar{a}^2 - 1) \quad (3.21)$$

where the branch of the square root is chosen so that  $0 < \arg(\cdot)^{1/2} < \pi$ .

We consider the seven domains which correspond respectively to the values  $a= 1.04, 1.08$  and  $a = 1.2(0.2)2.0$  and, in each case, we

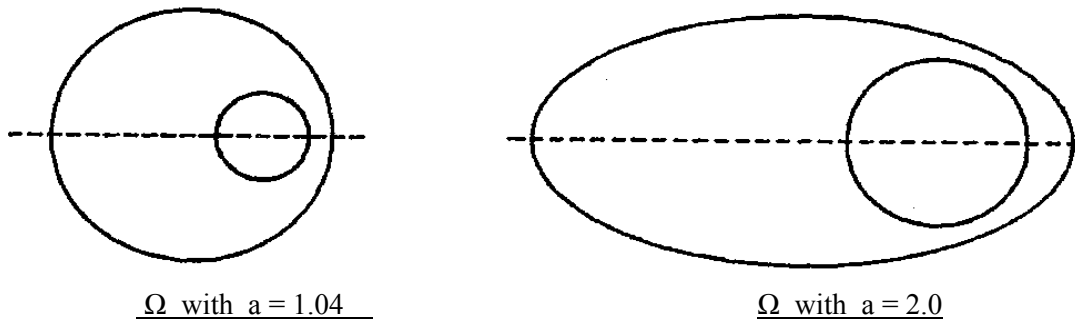


FIGURE 3.1

determine numerically the common symmetric points with respect to  $r_1$  and  $r_2$  by using the function  $S_2 = I_2 \circ I_2$ . More precisely, since any fixed points of  $S_2$  are zeros of the quartic polynomial,

$$Q(z) = \sum_{j=0}^4 b_j z^j, \quad \left. \begin{array}{l} \\ \\ \\ \\ \end{array} \right\} \quad (3.22)$$

$$b_0 = a^4(a^2 - 1)/81, b_1 = 2a^3/9, b_2 = a^2(25 - 2a^3)/9, b_3 = -2a, b_4 = a^2 - 1,$$

we determine the common symmetric points by solving numerically the equation

$$Q(z) = 0. \quad (3.23)$$

This leads to the following results: For each of the values  $a = 1.04, 1.08$  the Eq. (3.23) has four real roots, two of which are fixed points of  $S_2$ . Thus, for each



of these values of a, there is one pair of real common symmetric points  $\zeta_1 \in \text{Int}((\partial\Omega_1))$  and  $\zeta_2 = a^2/9\zeta_1 \in \text{Ext}((\partial\Omega_2).)$  The computed values of  $\zeta_1$  are listed in Table 3.1.

(ii) For each of the values a=1.2(0.2)2.0 the Eq. (3.23) has two pairs of complex conjugate roots, all of which are fixed points of  $S_2$ . Therefore, for each of these values of a, there are two pairs of complex common symmetric points  $\zeta_1, \zeta_2$  and  $\bar{\zeta}_1, \bar{\zeta}_2$  where  $\zeta_1 \in \text{Int}(\partial\Omega_1)$ ,  $\zeta_2, \bar{\zeta}_2 \in \text{Ext}(\partial\Omega_2)$  and  $\zeta_2 = a^2/9\bar{\zeta}_1$ . The computed values of  $\zeta_1$  are listed in Table 3.1.

TABLE 3.1

a	$\zeta_1$									
1.04	0.092	993	479	887						
1.08	0.090	844	724	819						
1.2	0.057	522	976	644	+ i	0.011	768	596	709	
1.4	0.068	995	111	309	+ i	0.077	804	537	657	
1.6	0.081	566	371	190	+ i	0.133	874	647	455	
1.8	0.095	912	475	177	+ i	0.198	980	792	698	
2.0	0.113	004	586	098	+ i	0.279	182	238	643	

3.2 Circular domain with a "cardioid shaped" hole

Let  $\Omega$  be the doubly-connected domain whose interior and exterior boundaries are respectively

with

$$\left. \begin{aligned} \partial\Omega_1 &= \{Z : Z = T_1(S), \quad -\pi < S \leq \pi\}, \\ T_1(s) &= \{0.5 + \cos(s/2)\}e^{is}, \end{aligned} \right\} \quad (3.24)$$

and

$$\partial\Omega_2 = \{z : |z| = a, \quad a > 1.5\} ; \quad (3.25)$$

see Fig 3.2. As in the previous example we take  $\Gamma_j = \partial\Omega_j$ ;  $j=1,2$ .

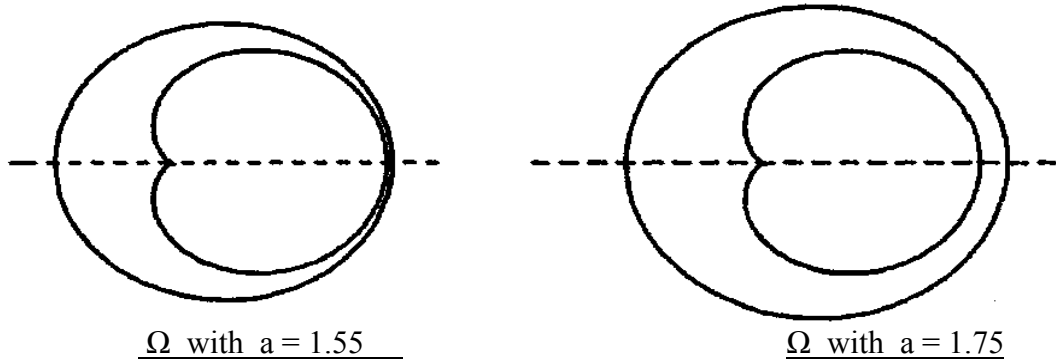


FIGURE 3.2

In this case the formula  $I_1(z) = \overline{\tau_1\{\tau_1^{[-1]}(z)\}}$ , for the symmetric Point with respect to  $\Gamma_1$ , cannot be written down explicitly. However, For any real value of  $t$ ,

$$\tau_1(\pm it) = \{0.5 + \cosh(t/2)\}^{\mp t} \quad (3.26)$$

defines two real symmetric point with respect to  $r_1$  and these are common symmetric with respect to  $r_1$  and  $r_2$  provided that the parameter  $t$  satisfies the equation.

$$\tau_1(it) \cdot \tau_1(-it) = a^2,$$

i.e

$$0.5 + \cosh(t/2) = a \quad (3.27)$$

Since the equation (3.27) has roots

$$\begin{aligned}
t &= 2 \cosh^{-1}(a - 0.5) \\
&= \pm 2 \log b; \quad b = a - 0.5 + \{(a - 0.5)^2 - 1\}^{\frac{1}{2}}, \\
(3.28)
\end{aligned}$$

It follows that there is one pair of real common symmetric points

$\zeta_1 \in \text{Int}(\partial\Omega_1)$  and  $\zeta_2 \in \text{Ext}(\partial\Omega_2)$  where

$$\zeta_1 = a/b^2 \quad \text{and} \quad \zeta_2 = ab^2.$$

(3.29)

#### 4. Numerical Conformal Mappings

In this section we illustrate how the information regarding the singularities of the analytic extension of  $H$  may be used to improve the efficiency of certain numerical conformal mapping techniques. We do this by presenting a number of numerical examples, involving the mapping of the domains considered in Sections 2 and 3. In each example, the approximation to the mapping function  $f$  is computed by using the orthonormalization method (ONM), considered recently in [5]. The ONM emerges easily from the theory contained in [2,p.249], [1,p.102] and [4,p.373]. The details of the method are as follows.

Let  $L_2(\Omega)$  be the Hilbert space of all square integrable functions which are analytic and possess a single-valued indefinite integral in  $\Omega$ , and denote the inner product of  $L_2(\Omega)$  by  $(\cdot, \cdot)$ , i.e.

$$g_1, g_2 = \int_{\Omega} g_1(z) \overline{g_2(z)} dx dy. \quad (4.1)$$

Then it is shown in [2,p.250] that, for each function  $\eta \in L_2(\Omega)$

$$(n.H) = i \int_{\partial\Omega} \eta(z) \log|z| dz,$$

(4.2)

where  $H$  is the function defined by (1.3). It is also shown in [2] that the modulus  $M$  of  $\Omega$  is related to  $H$  by means of

$$\log M = \left\{ \frac{1}{i} \int_{\partial\Omega} \frac{1}{z} \log|z| dz - \|H\|^2 \right\} / 2\pi ,$$

(4.3)

where  $\|H\|^2 = (H, H)$ .

Let  $\{\eta_j(z)\}$  be a complete set of  $L_2(\Omega)$ . Then the result (4.2) suggests the following procedure for obtaining a numerical approximation

to the mapping function  $f$ . The set  $\{\eta_j(z)\}_{j=1}^N$  is orthonormalized by

means of the Gram-Schmidt process to give the orthonormal set  $\{\eta_j^*(z)\}_{j=1}^N$ ,

and the function  $H$  is approximated by the finite Fourier series sum

$$H_N(z) = \sum_{j=1}^N \beta_j \eta_j^*(z) , \quad (4.4)$$

where the Fourier coefficients

$$\beta_j = (H, \eta_j^*) ,$$

(4.5)

are known by means of (4.2). Then, because of (1.3) and (4.3),

$$f_N(z) = \frac{1}{t} z \exp \left\{ \int_t^z H_N(\zeta) d\zeta \right\}$$

(4.6)

and

$$M_N = \exp \left\{ \left( \frac{1}{i} \int_{\partial\Omega} \log|z| dz - \|H_N\|^2 \right) / 2\pi \right\} , \quad (4.7)$$

give respectively the  $N$ th ONM approximations to the mapping function  $f$  and to the modulus  $M$  of  $\Omega$ . Clearly,

$$\lim_{N \rightarrow \infty} \|H_N - H\| = 0 \quad (4.8)$$

and, in the space  $L_2(\Omega)$ , this norm convergence implies that  $H_N(z) \rightarrow H(z)$  for  $N \rightarrow \infty$  in every compact subset of  $\Omega$

The information regarding the singularities of the analytic extension

of  $H$  is needed for selecting the set of basis functions  $\{\eta_j(z)\}$  so that the resulting approximating series (4.4) converges rapidly. This is an essential requirement for the successful application of the ONM, because the Gram-Schmidt process is numerically unstable. The significance of the results of Sections 2 and 3 emerges from the observation that rapid convergence can be achieved by using an "augmented basis", formed by introducing into the "monomial set"

$$\{z^j\}_{j=-\infty}^{\infty}, \quad j \neq -1, \quad (4.9)$$

functions that reflect the main singularities of  $H$  on  $\partial\Omega$  and in  $\text{comp}1(\overline{\Omega})$ ; see [5,Sect.4].

The problem of constructing an augmented basis for dealing with any corner singularities that  $H$  may have on  $\partial\Omega$  is studied fully in [5].

Here we are concerned only with the treatment of singularities in  $\text{comp}1(\overline{\Omega})$ , and the purpose of the examples presented below is to illustrate the importance of introducing into the basis set functions that reflect the singular behaviour of  $H$  at common symmetric points with respect to

$\partial\Omega_1$  and  $\partial\Omega_2$ . The form of these singular functions is suggested by the results of the previous sections. Thus, if the domain under consideration has common symmetric points at  $\zeta_1 \in \text{Int}(\partial\Omega_1)$  and  $\zeta_2 \in \text{Ext}(\partial\Omega_2)$  then, in order to reflect the singularities of  $H$  at these two points, we introduce into the set (4.9) the functions

$$\eta_1(z) = 1/(z-\zeta_1) - 1/z \quad (4.10)$$

and

$$\eta_2(z) = 1/(z-\zeta_2) \quad (4.11)$$

(The term  $-1/z$  is included in (4.10) so that the function  $\eta_1$  has a single-valued integral in  $\Omega$ ).

The computational details of the ONM procedure used in the numerical examples are as described in [5,Sect,5]. In particular, the estimate  $E_N$  of the maximum error in  $\{f_N(z)\}$  is given, as in [5], by the quantity

$$E_N = \max \left\{ \max_j \left| |f_N(z_j^{(1)})| - 1 \right|, \max_j \left| |f_N(z_j^{(2)})| - M_N \right| \right\} \quad (4.12)$$

where  $\{z_j^{(1)}\}$  and  $\{z_j^{(2)}\}$  are two sets of "boundary test points" on  $\partial\Omega_1$  and  $\partial\Omega_2$  respectively. We expect (4.12) to be a reasonable estimate because in general, the approximation  $M_N$  to the modulus  $M$  of  $f$  is more accurate than  $|f_N(z)|$ ,  $z \in \partial\Omega$ ; see e.g. the numerical results in [5,Sect.6].

In presenting the results we adopt the notation used in [5], and denote the ONM with monomial basis (4.9) by ONM/MB and the ONM with augmented basis by ONM/AB. Also, in each example, the numerical results correspond to the approximation  $f_{N_{\text{opt}}}$ , where  $N = N_{\text{opt}}$  is the "optimum number" of basis functions which gives maximum accuracy in a sense similar to that described in [5,Sect.5].

All computations were carried out on a CDC7600 computer, using programs written in FORTRAN with single precision working. Single length working on the CDC7600 is between 13 and 14 significant figures.

#### Example 4.1

Let  $\Omega$  be the domain considered in Section 2. That is,  $\Omega$  is bounded internally by the circle

$$\partial\Omega_1 = \{z : |z| = a, a < 1\}$$

and externally by the  $n$ -sided regular polygon

$$\partial\Omega_2 = \bigcup_{j=1}^n \gamma_j,$$

where

$$\gamma_j = \Gamma_2 \omega^{j-1}, \quad \omega = \exp\{2\pi i/n\}; \quad j=1,2,\dots,n,$$

and  $\gamma_1 = \Gamma_2$  is the side given by (2.2).

In this case there are  $n$ -pairs of common symmetric points associated with  $\partial\Omega_1$  and each of the sides  $\gamma_j$ ;  $j=1,2,\dots,n$  of  $\partial\Omega_2$ . These points are respectively

$$\zeta_1^{(j)} = \zeta_1 \omega^{j-1} \quad \text{and} \quad \zeta_2^{(j)} = \zeta_2 \omega^{j-1}; \quad j=1,2,\dots,n, \quad (4.13)$$

where  $\zeta_1^{(1)} = \zeta_1$  and  $\zeta_2^{(1)} = \zeta_2$  are defined by (2.12).

Because the domain has  $2n$ -fold symmetry about the origin, the monomial basis set is taken to be

$$z^{(nj-1)}; \quad j = \pm 1, \pm 2, \dots. \quad (4.14)$$

Also, because of the symmetry, the  $n$ -pairs of singular functions (4.10)-(4.11), corresponding to the common symmetric points (4.13), can be combined into the two functions

$$\eta_1(z) = nz^{n-1}/(z^n - \zeta_1^n) - n/z, \quad (4.15)$$

and

$$\eta_2(z) = nz^{n-1}/(z^n - \zeta_2^n). \quad (4.16)$$

We consider first the case where  $n=3$ , i.e. the case where  $\partial\Omega_2$  is an equilateral triangle, and in Table 4.1 we list the computed values of  $E_{N_{\text{opt}}}$  corresponding respectively to circular holes of radii  $a = 0.1, 0.2, 0.5, 0.9, 0.95, 0.99$  and  $0.995$ . (In presenting the numerical re-

sults we use throughout the abbreviation  $x(-M)$  to denote  $x10^{-M}$  .)



TABLE 4.1

Equilateral triangle with circular hole

a	ONM/MB		ONM/AB	
	Nopt	$E_{\text{Nopt}}$	Nopt	$E_{\text{Nopt}}$
0.1	23	5.0(-7)	5*	6.7(-4)
0.2	21	2.6(-7)	5*	6.9(-4)
0.5	21	4.2(-7)	21	3.7(-8)
0.9	21	1.2(-4)	21	2.2(-7)
0.95	29	8.8(-4)	20	1.7(-7)
0.99	25	1.2(-2)	25	3.7(-7)
0.995	23	1.8(-2)	15	2.4(-6)

\* The Gram-Schmidt process breaks down when  $N = 6$ .

In the two cases  $a = 0.1$  and  $a = 0.2$  the ONM/AB breaks down after only a few applications of the Gram-Schmidt process. The reason for this is that the function  $\eta_1$ , given by (4.15) with  $n = 3$ , has the series expansion

$$\eta_1(z) = (3/\zeta_1) \sum_{j=1}^{\infty} (\zeta_1/z)^{3j+1}, \quad |z| > \zeta_1,$$

which for small  $a$  converges rapidly in  $\Omega$ . This means that there is "near" linear dependence between  $\eta_1$  and the first few "negative" monomials

$$z^{-(3j+1)}; \quad j = 1, 2, \dots,$$

(4.17)

and, for this reason, severe ill-conditioning occurs. One way of partly overcoming this difficulty is to omit from the augmented basis the first term of (4.17), i.e. the term  $z^{-4}$ . If this approach is adopted then the ONM/AB gives

$$\begin{aligned} \text{Nopt} = 18, & & E_{18} = 3.1 \times 10^{-8}, \\ (4.18) & & \end{aligned}$$

when  $a = 0.1$ ,

$$\begin{aligned} \text{Nopt} = 18, & & E_{18} = 1.5 \times 10^7, \\ (4.19) & & \end{aligned}$$

when  $a = 0.2$ , and

$$\begin{aligned} \text{Nopt} = 18, & & E_{18} = 3.1 \times 10^{-8}, \\ (4.20) & & \end{aligned}$$

when  $a = 0.5$ .

The results of Table 4.1, together with (4.18)-(4.19) and results for other values of  $a$  not presented here, indicate that, when  $n = 3$ , the use of an augmented basis containing the functions (4.15)-(4.16) always leads to improved approximations. This is so, provided that the near linear dependence of  $\eta_1$  mentioned above is taken into account, and when  $a$  is small the monomial  $z^{-4}$  is omitted from the basis. However, our results show that the improvement achieved by the ONM/AB is considerable only when the radius  $a$  of  $\partial\Omega_1$  is close to unity. For all other values of  $a$  the accuracy of the ONM/MB is good and there is no real need for using an augmented basis.

The above observations, concerning the significance of the singular basis functions  $\eta_1$  and  $\eta_2$  in the case  $n = 3$ , also apply to the mapping of domains whose outer boundary  $\partial\Omega_2$  is a polygon with  $n > 3$  sides. In other words, for any  $n$ , the effect of the singularities of  $H$  at the common symmetric points (4.13) is serious only when the radius of  $\partial\Omega_1$  is close to unity. This is certainly so when  $n = 4$ , i.e. when  $\Omega$  is a square with a circular hole. In this case, because of the increased symmetry, the ONM/MB results are substantially more accurate than those listed in Table 4.1. For example, when  $a = 0.2, 0.4$  and  $0.8$  the ONM/MB gives respectively

$$E_{20} = 9.5 \times 10^{-12}, \quad E_{22} = 3.1 \times 10^{-12} \quad \text{and} \quad E_{28} = 1.8 \times 10^{-10};$$

see [5,Ex.5.1]. If  $n > 4$  then the function  $H$  has a branch point singularity at each of the  $n$  corners of  $\partial\Omega_2$ . These corner singularities are always serious and, for this reason, when  $n > 4$  the augmented basis must always contain "corner" singular functions of the type described in [5]. For most values of  $a$ , high accuracy is achieved by using an augmented basis formed by introducing only corner singular functions into the set (4.14).

The inclusion of the functions  $\eta_1$  and  $\eta_2$  leads to improved approximations only when  $a$  is very close to unity. Thus, in general, the need for reflecting the singularities of  $H$  at the common symmetric points arises only when the hole of the polygonal domain under consideration is large. Such domains are apparently of practical significance, in connection with certain elasticity problems for infinite plates having doubly periodic distributions of closely spaced holes; see e.g. [7,p.318].

In order to illustrate the above remarks we consider the mapping of  $\Omega$  in the two cases where  $n = 4$  and  $n = 5$ , i.e. where  $\partial\Omega_2$  is a square and a pentagon. The computed values of  $E_{\text{Nopt}}$ , corresponding to circular holes of radii  $a = 0.9, 0.99$  and  $0.999$ , are listed in Tables 4.2 and 4.3. In the case of the pentagonal domain the results ONM/AB, in Table 4.3, are obtained by using a basis formed by introducing into the set (4.14) the functions  $\eta_1, \eta_2$  and also a corner singular function  $\tilde{\eta}$ , whose purpose is to reflect the corner singularities of  $H$ . The results ONM/ $A\tilde{B}$ , which are also listed in Table 4.3, are obtained by using as basis the monomial set (4.14) augmented by introducing the corner singular function  $\tilde{\eta}$  only.

The results of Tables 4.2 and 4.3 illustrate the significant improvement in accuracy that can be achieved when  $a$  is very close to unity, by introducing into the basis set the singular functions  $\eta_1$  and  $\eta_2$ . The results

TABLE 4.2  
Square with circular hole

a	ONM/MB		ONM/AB	
	Nopt	$E_{\text{Nopt}}$	Nopt	$E_{\text{Nopt}}$
0.9	25	4.7(-8)	17	3.0(-8)
0.99	25	1.9(-3)	23	1.8(-9)
0.999	27	1.7(-2)	11	1.3(-5)

TABLE 4.3  
Pentagon with circular hole

a	ONM/MB		ONM/ $\tilde{A}\tilde{B}$		ONM / AB	
	Nopt	$E_{\text{Nopt}}$	Nopt	$E_{\text{Nopt}}$	Nopt	$E_{\text{Nopt}}$
0.9	30	4.6(-5)	24	2.5(-10)	18	1.7(-9)
0.99	26	1.8(-5)	30	1.2(-5)	25	1.4(-10)
0.999	27	5.5(-3)	28	4.3(-3)	25	1.5(-10)

also show that the ONM/MB or, if  $n > 4$ , the ONM/ $\tilde{A}\tilde{B}$  achieve high accuracy even when the radius of the hole is as large as  $a = 0.9$ . In fact, in the case  $a = 0.9$  of the pentagonal domain the  $E_{\text{Nopt}}$  corresponding to the ONM/ $\tilde{A}\tilde{B}$  is less than that of the ONM/AB. This is due to greater instability, caused by the introduction of the function  $\eta_1$  into the basis set.

Theorem 2.2 and the discussion which led to this theorem suggest that, in the ONM/AB, the coefficients  $c_1$  and  $c_2$  of the singular functions  $\eta_1$  and  $\eta_2$  might be close to  $\pm r_1$ , respectively, where  $r_1$  is given by (2.33). In order to test this, we list in Tables 4.4-4.6 the computed coefficients

$c_1$  and  $c_2$  and we compare them with the value  $r_1$ , which we compute from (2.33), by using the best available approximation  $M_{N_{\text{opt}}}$  to the conformal modulus  $M$  of  $\Omega$ . In each table we also list the values of  $M_{N_{\text{opt}}}$  used for determining  $r_1$ .

TABLE 4.4

Equilateral triangle with circular hole

a	$M_{N_{\text{opt}}}$	$R_1$	$c_1$	$c_2$
0.1	11.320 933 159	0.810 716	0.912 058	-0.941 970
0.2	5.660 452 463	0.756 186	0.891 406	-0.811 842
0.5	2.262 776 769	0.620 060	0.751 555	-0.526 729
0.9	1.222 664 205	0.430 342	0.424 505	-0.429 393
0.95	1.137 027 112	0.397 531	0.397 566	-0.397 259
0.99	1.052 393 003	0.359 587	0.359 587	-0.359 578
0.995	1.035 851 938	0.351 507	0.351 449	-0.351 492

TABLE 4.5

Square with circular hole

a	$M_{N_{\text{opt}}}$	$R_1$	$c_1$	$c_2$
0.9	1.184 090 961	0.361 719	0.397 421	-0.358 626
0.99	5.040 412 137	0.278 964	0.278 964	-0.278 963
0.999	1.011 633 061	0.258 514	0.258 611	-0.258 609

TABLE 4.6

Pentagon with circular hole

a	$M_{N_{\text{opt}}}$	$r_1$	$c_1$	$c_2$
0.9	1.162 649 997	0.322 602	0.410 822	-0.344 350
.99	1.033 311 414	0.230 741	0.230 739	-0.230 743
0.999	1.009 390 376	0.208 908	0.208 908	-0.208 908

It is gratifying to observe that the results of the above tables con-firm the prediction which emerged from Theorem 2.3. That is, the agreement between the computed coefficients  $c_1$  and  $c_2$  and the values  $\pm r_1$  increases with  $a$ , and there is close agreement when  $a$  is close to unity. (In Table 4.5, the agreement between  $c_1$ ,  $c_2$  and  $\pm r_1$  when  $a = 0.999$  is not as close as when  $a = 0.99$ . This is due to the fact that the accuracy of the ONM/AB approximations when  $a = 0.999$  is considerably worse than when  $a = 0.99$ ; see Table 4.2.)

Finally, we note that the values of  $r_1$  listed in Tables 4.4-4.6 satisfy the inequality (2.56) and, as might be expected, when  $a$  is close to unity both  $\hat{\beta} = \pi/n\beta$  and  $\hat{\alpha} = \pi/n\alpha$  are close to  $r_1$ . For example, in the case  $n = 5$  and  $a = 0.999$  we find that

$$\hat{\beta} = 0.208144 \quad \text{and} \quad \hat{\alpha} = 0.209151 .$$

Example 4.2

Let  $\Omega$  be the domain defined in Section 3.1, whose boundary components are respectively the circle  $\partial\Omega_1$  and the ellipse  $\partial\Omega_2$  given by (3.19).

We consider the mapping of  $\Omega$  in the seven cases where  $a = 1.04, 1.08$  and  $1.2(0.2)2.0$  and recall that, depending on the value of  $a$ , there are either one real pair  $\zeta_1, \zeta_2$  or two complex pairs  $\zeta_1, \zeta_2$  and  $\bar{\zeta}_1, \bar{\zeta}_2$  of common symmetric points with respect to  $\partial\Omega_1$  and  $\partial\Omega_2$ ; see Table 3.1 for the values of  $\zeta_1$ . Thus, the augmented basis is formed by introducing into the monomial set (4.9) either two or four singular functions of the form (4.10) - (4.11). The computed values of  $E_{\text{Nopt}}$  obtained by using the ONM/MB and the ONM/AB are listed in Table 4.7. These results show that considerable improvement in accuracy is achieved by the ONM/AB in the cases where  $a$

is close to two or to unity, i.e. when  $\partial\Omega_1$  is "close" to  $\partial\Omega_2$  or  $\partial\Omega_2$  is nearly circular.

TABLE 4.7

A	ONM/MB		ONM/AB	
	Nopt	$E_{\text{Nopt}}$	Nopt	$E_{\text{Nopt}}$
1.04	31	2.1(-5)	30	1.0(-8)
1.08	31	8.7(-6)	21	9.7(-8)
1.20	29	7.5(-8)	19	6.1(-8)
1.40	29	2.0(-6)	23	1.9(-7)
1.60	25	3.2(-5)	25	5.6(-7)
1.80	23	3.9(-4)	19	7.6(-6)
2.00	27	2.0(-3)	25	2.7(-6)

In Table 4.8 we list the computed approximations  $E_{\text{Nopt}}$  to the modulus  $M$  of  $\Omega$ , the computed coefficients  $c_1$  and  $c_2$  of the two singular functions corresponding to the points  $\zeta_1$  and  $\zeta_2$  and the values  $r_1$ , which we determine from (3.18) by using the approximations  $E_{\text{Nopt}}$  instead of  $M$ . The purpose of this table is to test whether the coefficients  $c_1, c_2$  are close to  $r_1, -\bar{r}_1$ .

TABLE 4.8

a	$E_{\text{Nopt}}$	$r_1$	$c_1$	$c_2$
1.04	2.081 686 626	1.020	0.399	-1.020
1.08	2.053 744 500	1.052	1.011	-1.053
1.20	1.968 317 921	0.839 - i 1.048	0.216 - i 0.863	-0.925 - i 0.990
1.40	1.824 572 938	0.703 - i 0.194	0.391 - i 1.092	-0.705 - i 0.214
1.60	1.683 966 719	0.673 - i 0.111	0.728 - i 0.103	-0.671 - i 0.117
1.80	1.549 091 634	0.647 - i 0.071	0.640 - i 0.073	-0.641 - i 0.078
2.00	1.419 684 616	0.620 - i 0.046	0.621 - i 0.044	-0.620 - i 0.046

The overall behaviour of the results of Table 4.8 is rather erratic and, for this reason, it is difficult to reach any precise conclusions regarding the coefficients  $c_1$  and  $c_2$ . We observe however that there is closer agreement between the values  $c_2$  and  $-\bar{r}_1$  than there is between the values  $c_1$  and  $r_1$ . More specifically, there is always some agreement between  $c_2$  and  $-\bar{r}_1$ , whilst when  $a = 1.04, 1.20$  and  $1.40$  there is no agreement at all between  $c_1$  and  $r_1$ . This is probably due to the numerical instability of the method. We also observe that the results of Table 4.8 resemble those of Tables 4.4-4.6, in the sense that the agreement between the computed coefficients and the values  $r_1, -\bar{r}_1$ , tends to be closer in the cases where the ONM/AB produces considerably more accurate approximations than the ONM/MB.

#### Example 4.3

Let  $\Omega$  be the domain defined in Section 3.2, whose boundary components  $\partial\Omega_1$  and  $\partial\Omega_2$  are given by (3.24) and (3.25).

In this case, for any value of the radius  $a$  of  $\partial\Omega_2$ , there is only one pair of real common symmetric points  $\zeta_1, \zeta_2$  with respect to  $\partial\Omega_1$  and  $\partial\Omega_2$ . Thus, for any value of  $a$ , the augmented basis is formed by introducing into the monomial set (4.9) the two singular functions (4.10)-(4.11), where  $\zeta_1$  and  $\zeta_2$  are given by (3.28) -(3.29).

The numerical results obtained for the four cases where  $a = 1.51, 1.55, 1.60$  and  $1.75$  are listed in Table 4.9. These results illustrate the very considerable improvement in accuracy which is achieved by the M/AB when the radius of  $\partial\Omega_2$  is close to 1.5, i.e. when  $\partial\Omega_1$  is "close" to  $\partial\Omega_2$ .



TABLE 4.9

a	ONM/MB		ONM/AB	
	Nopt	$E_{\text{Nopt}}$	Nopt	$E_{\text{Nopt}}$
1.51	30	2.0(-2)	28	3.9(-10)
1.55	28	3.1(-4)	28	5.7(-10)
1.60	30	1.3(-5)	26	2.3(-9)
1.75	28	6.8(-8)	26	1.7(-9)

In Table 4.10 we list the value of  $M_{\text{Nopt}}$ , the computed coefficients  $c_1, c_2$  of the two singular functions  $\eta_1, \eta_2$ , and the values  $r_1$  which, as in Ex. 4.21, we determine from (3.18) by using the approximations  $M_{\text{Nopt}}$  instead of  $M$ . For the four values of  $a$  considered, our results show that there is always some agreement between  $c_1, c_2$  and  $r_1, -r_1$  and that the agreement is excellent when  $a$  is close to 1.5. Thus, the entries of Table 4.10 display the same behaviour as those of Tables 4.4-4.6 and 4.8, in the sense that the agreement between  $c_1, c_2$  and  $r_1, -r_1$  is closer in the cases where the ONM/AB leads to considerably improved approximations,

TABLE 4.10

a	$M_{\text{Nopt}}$	$r_1$	$C_1$	$c_2$
1.51	1.051 456 961	1.068 052 0	1.068 052 0	-1.068 052 0
1.55	1.128 173 218	1.163 576 0	1.163 573 6	-1.163 564 3
1.60	1.196 339 075	1.243 205 8	1.243 188 1	-1.244 268 8
1.75	1.362 121 219	1.419 850 1	1.422 547 3	-1.372 296 4

5. Discussion

Our remarks, concerning the improvement in accuracy achieved by introducing into the basis set singular functions of the form (4.10) -(4.11), also apply to the other expansion methods for the numerical conformal mapping of doubly-connected domains. For example, precisely the same remarks hold in connection with the use of the variational method of Gaier [2,p.249], the numerical implementation of which is considered in [5],

Acknowledgement

We are grateful to Professor D. Gaier for many invaluable comments and suggestions. One of us (N.P.) is also grateful to Dr. D. Levin for several helpful discussions on the problem of determining the singularities of the mapping function for doubly-connected domains.

K LOAN

REFERENCES

1. Bergman, S.: The kernel function and conformal mapping. Math. Surveys 5, Am. Math. Soc, Providence R.I. (2nd ed.) 1970.
2. Gaier, D.: Konstruktive Methoden der konformen Abbildung. Berlin-Heidelberg-New York: Springer 1964.
3. Henrici, P.: Applied and Computational Complex Analysis, Vol.11. New York: Wiley 1977.
4. Nehari, Z.: Conformal Mapping. New York: McGraw-Hill 1952.
5. Papamichael, N., Kokkinos, C.A. : The use of singular functions for the approximate conformal mapping of doubly-connected domains.  
To appear in: SLAM J. Sci. Stat. Comput.
- 6 Papamichael, N., Warby, M.K., Hough, D.M.: The determination of thepoles  
of the mapping function and their use in numerical conformal mapping. To appear in: J. Comp. and Appl. Maths.
7. Richardson, M.K., Wilson, H.B.: A numerical method for the conformal mapping of finite doubly-connected domains. Develop. Theoret.. Appl. Mech. 3, 305-321 (1967).
8. Sansone, G., Gerretsen, J.: Lectures on the theory of functions of a complex variable, Vol.11. Groningen: Walters-Noordhoff 1969.

**NOT TO BE  
REMOVED**

FROM THE LIBRARY

XB 2356451 2

